Surface functionalisation of bacterial cellulose as the route to produce green polylactide nanocomposites with improved properties

Koon-Yang Lee, Jonny J Blaker, Alexander Bismarck*
Polymer and Composite Engineering (PaCE) group
Department of Chemical Engineering
Imperial College London, South Kensington Campus, SW7 2AZ, UK

Abstract

The effect of surface functionalisation of bacterial cellulose nanofibrils (BC) and their use as reinforcement for polylactide (PLLA) nanocomposites was investigated. BC was functionalised with various organic acids via an esterification reaction. This rendered the otherwise hydrophilic BC hydrophobic and resulted in better compatibility (interfacial adhesion) between PLLA and BC. A direct wetting method, allowing the determination of the contact angle of polymer droplets on a single BC nanofibre, was developed to quantify the interfacial adhesion between PLLA and functionalised BC. It was found that the contact angle between PLLA droplets and functionalised BC decreased with increasing chain lengths of the organic acids used to hydrophobise BC. A novel method to compound BC with PLLA based on thermally induced phase separation (TIPS) to yield a dry form of pre-extrusion composite was also developed. The mechanical properties of the surface functionalised BC reinforced PLLA nanocomposites showed significant improvements when compared to neat PLLA and BC reinforced PLLA. The thermal degradation and viscoelastic behaviour of the nanocomposites were also improved over neat PLLA.

Keywords: A. Nano composites, B. Mechanical properties, Bacterial cellulose, Esterification, Organic acid

* Corresponding author: Tel: +44 (0)20 7594 5578, Fax: +44 (0)20 7594 5638
Email address: a.bismarck@imperial.ac.uk

1. Introduction

Recent interest in greener polymeric materials for general applications such as packaging and the public's growing demand for environmentally friendlier products have sparked the development of green composite materials [1]. One of the most extensively studied renewable reinforcements in this field is cellulose. Cellulose is the most abundant natural polymer, found in plant cells walls, and synthesised by some bacteria and one sea animal (tunicate). The use of cellulosic materials in the production of green composites is well established. Numerous studies have focussed on the use of natural fibres in the production of composite materials [2-7]. More recently, our group [8, 9] has successfully deposited BC onto natural fibres, thereby creating hierarchical composites with improved mechanical properties. Extensive research in the field of natural fibre reinforced composite materials is not surprising as natural fibres have many distinct advantages over conventional glass fibres. These include low cost, low density, high toughness, biodegradability and most importantly, carbon neutrality [10, 11]. Major automotive companies in Germany such as Mercedes Benz and BMW have started to replace their glass fibre based composites with natural fibre reinforced plastics for their door panel and boot linings [12]. Rieter Automotive won the JEC Composites Award in 2005 for their development in natural fibre reinforced thermoplastic for an under-floor module with integrated aerodynamic, thermal and acoustic functions [13].

Cellulose derived from bacteria such as from the *Acetobacter* species [14] has the advantage of being free from wax, lignin, hemicellulose and pectin, which are present in plant-based cellulosic materials. BC is highly crystalline, with a degree of crystallinity of about 90% [15]. This highly crystalline structure of BC is a property that is favourable for composite production as it results in a high Young's modulus value for BC. It was found that BC possesses a Young's modulus of about 114 GPa and a theoretical Young's modulus of between 130 GPa to 145 GPa depending on the crystallinity [16]. This value is exceeds that of synthetic glass fibres (~70 GPa) and aramid fibres (~67 GPa), considering that BC has a lower density (1.25 g cm^{-3}) than glass fibres (2.5 g cm^{-3}). Natural fibres, on the other hand, possess much lower Young's moduli; cotton (12.6 GPa), jute (26.5 GPa), flax (27.6 GPa) and sisal (22 GPa), respectively [17]. Unlike natural fibres, which has to be microfibrillated to produce cellulose strands in the order of 1-100 nm in diameter [18], BC

exists naturally as a nano-sized material (between 24-86 nm in diameter and several micrometres in length) [14, 19] and it has a surface area of about 37 m^2 g^{-1} [20]. Such properties are highly advantageous for the production of composite materials as this implies that for the same amount of material, the interface between the matrix and the reinforcement will be larger for BC compared to micrometre-scale natural fibres. However, these interesting properties of BC do come with a price as BC is extremely hydrophilic in nature. As a result, BC will often have poor interfacial adhesion to hydrophobic polymer matrices such as polylactide [9]. However, it can be anticipated that the highly crystalline structure of BC can be retained when the surface of BC is hydrophobised. By preserving the crystalline structure of BC, the Young's modulus will not be affected much and by combining it with a biodegradable polymer, truly green nanocomposites can be produced.

Poly(L-Lactic Acid) (PLLA) is a biodegradable, hydrophobic aliphatic thermoplastic polyester, derived fully from renewable resources such as corn, starch or sugarcane. It belongs to the family of poly(α-hydroxy acids) and is degraded principally via hydrolysis and to a lesser extent either though enzymatic attack [2, 21]. PLLA has been used in biomedical applications but its application is somewhat limited by its inherently poor properties such as poor impact strength, low thermal stability and narrow processing window [22]. Modifications to PLLA are necessary so that it can compete with the conventional "big four" (PP, PE, PS, PVC) and other engineering polymers.

In this work we attempt to produce green nanocomposites using functionalised BC to improve the interfacial adhesion between BC and hydrophobic PLLA. BC was functionalised using various organic acids (acetic, hexanoic and dodecanoic acid). A direct wetting method was developed to determine the contact angle of PLLA on these surface functionalised BC. A method based on thermally induced phase separation (TIPS) was adapted from the literature [23] to produce composite microspheres which enables the compounding of dry BC in the polymer using conventional extrusion. The mechanical properties, thermal behaviour and viscoelastic properties of the nanocomposites were also characterised.

2. Experimental

2.1. Materials

PLLA was purchased from Biomer (L9000, MW ≥ 150 kg mol^{-1}, D-content ≈ 1.5%) and was used as the matrix for the production of nanocomposites. 1,4-Dioxane (Sigma-Aldrich, ACS Reagent, ≥ 99% purity) was used as the solvent for PLLA. Pyridine (analaR NORAMPUR, ≥ 99.7% purity), methanol (GPR, ≥ 99% purity), ethanol (GPR, ≥99% purity) and acetic acid (analaR, ≥ 99.8% purity) were purchased from VWR. Hexanoic acid (Aldrich, ≥ 99.5% purity), dodecanoic acid (Aldrich, ≥ 98% purity), dimethyl carbonate (Aldrich Reagent Plus, ≥ 99% purity) and *p*-toluenesulfonyl chloride (Aldrich, ≥ 99% purity) were purchased from Sigma-Aldrich. Sodium hydroxide (purum grade, pellets) was purchased from Acros Organics. All materials were used as received without further purification. BC was extracted from commercially available *Nata-de-coco* (CHAOKOH coconut gel in syrup, Ampol Food Processing Ltd, Nakorn Pathom, Th).

2.2. Extraction and purification of BC

BC was extracted from *Nata-de-coco* in batches of 5 jars (of net weight 500 g each). For each batch of 5 jars, the coconut gels content was rinsed 3 times with 5 L of de-ionised water and blended for 1 min using a laboratory blender (Waring Blender LB20EG, Christison Particle Technologies, Gateshead, UK). The blended BC was then homogenised at 20,000 rpm in 5 L of water for 2 min using a homogeniser (Polytron PT 10-35 GT, Kinematica, CH) and centrifuged at 14,000g to remove excess water. In order to purify the BC, the centrifuged BC was re-dispersed in 5 L of de-ionised water and heated in 0.1 M NaOH solution at 80°C for 20 min to remove any remaining microorganisms and soluble polysaccharides [24]. The purified BC was then successively centrifuged and homogenised to neutral pH.

2.3. Surface functionalisation of BC

A functionalisation protocol, developed for the modification of natural fibres was adapted from the literature [25, 26] and modified to suit the derivatisation of BC. A dry weight equivalent of 2 g of the purified BC (wet) was solvent exchanged from water through methanol into pyridine at a concentration of 0.3% (g mL^{-1}) to ensure the complete removal of water and methanol. The mixture was homogenised at 20,000 rpm for at least 1 min at each stage to completely disperse BC in the solvent. BC was retained through centrifugation at 14,000g for 15 min prior re-dispersion in the subsequent solvent. The solvent exchange method was used in this case due to the inability of (vacuum) dried BC to

re-disperse in any medium because of the strong hydrogen bonds that formed between the nanofibrils. In the final solvent exchange step, the concentration of BC in pyridine was adjusted to 0.5% (g mL^{-1}). From the authors' experiences, this is the concentration at which the mixture can still be stirred properly. At higher concentrations, the mixture becomes too viscous to stir. This BC-pyridine mixture was poured into a 1 L 3-neck round bottom flask and stirred using a magnetic stirrer. 92 g (0.48 mol) of *p*-toluenesulfonyl chloride was added into the reaction vessel and an equimolar amount of organic acids was added into the vessel after the addition of *p*-toluenesulfonyl chloride. The reaction was conducted for 2 h at 50°C under nitrogen flow to create an inert atmosphere such that water vapour does not affect the esterification reaction. After the reaction, the reaction medium was subsequently quenched with 1.5 L of ethanol and washed 3 times with 800 mL of ethanol using the previously described homogenisation-centrifugation steps. The product was solvent exchanged from ethanol to water using this method. In order to use the BC in later stages, the product was freeze-dried. Neat and functionalised BC were dispersed in water and dimethyl carbonate respectively at a concentration of 0.4% (g mL^{-1}), flash frozen in Petri-dishes by immersion in liquid nitrogen and subsequently freeze-dried (Edwards Modulyo freeze dryer, UK). The BC functionalised with acetic, hexanoic and dodecanoic acid were termed C_2-BC, C_6-BC and C_{12}-BC, respectively.

2.4. Direct wetting measurement of functionalised BC

In order to investigate the wettability of individual functionalised BC by PLLA melts, a method developed to study the wetting of carbon nanotubes by polymers was adapted from the literature [27]. Approximately 4.4 mg of PLLA was dissolved in 5 mL of chloroform (0.06 wt%). The solution was left overnight to ensure PLLA fully dissolved in the solvent. Another suspension was prepared by dispersing 3.7 mg of BC in 5 mL of chloroform (0.05 wt%). This suspension was homogenised for 2 min at 20,000 rpm. The polymer solution was then added into this suspension and the resulting mixture homogenised again for 2 min at 20,000 rpm followed by ultrasonication for 1 h in a low powered ultrasonic bath to ensure adequate nanofibril dispersion. The mixture of PLLA and BC was added drop wise slowly into a 200 mL hexane/chloroform non-solvent bath (80:20 by weight) under magnetic stirring to precipitate PLLA onto individual cellulose nanofibrils. Precipitates were filtered using a PTFE membrane (0.2 μm pore size, Sartorius

Stedium Biotech, UK). The filter cake was heated for 30 min at 180°C while it is still on the PTFE membrane to melt to polymer. This filter cake was then investigated using a high resolution scanning electron microscope (LEO Gemini 1525 FEG-SEM, Oberkochen, D). The contact angles of the polymer droplets on the cellulose nanofibrils were determined using the generalised height-length method described in literature [28].

2.5. Preparation of composite microspheres with 2 wt% and 5 wt% BC loading

Most BC reinforced polymer composites fabrication methods reported in the literature are based on the solution casting method [11, 29-31]. Whereby, dry BC sheets are immersed in to polymer solutions and a composite is obtained by evaporation of the polymer solvent. In this work, a novel method based on TIPS [23] to produce composite microspheres was exploited. This method enables the homogeneous dispersion of dry BC in a polymer melt using conventional extrusion processes at later stages. 153 mg (2 wt%) and 395 mg (5 wt%) of freeze-dried BC were added into 90 mL of 1,4-dioxane, respectively and homogenised at 20,000 rpm to disperse them in 1,4-dioxane. PLLA pellets (7.5 g) were added into each mixture and left to dissolve overnight at 60°C under magnetic stirring. The resulting mixture was then poured into a 50 mL syringe and added drop wise into a bath of liquid nitrogen to rapidly induce the phase separation. The precipitates were collected in a 500 mL round bottom flask and subsequently freeze-dried to yield porous composite microspheres.

2.6. Processing of composite microspheres and the production of nanocomposite films

The produced composite microspheres with the desired weight fraction of BC were fed into a twin-screw micro-extruder (5 cm^3 micro-extruder, DSM research BV, NL) kept at a melt temperature of 180°C and a screw rotational speed of 10 rpm. After the addition of all the microspheres, the screw speed was increased to 40 rpm for 30 min to promote mixing of BC in the polymer melt. Finally, the polymer melt was extruded at a screw rotation speed of 20 rpm. These extrudates were pelletised and compression moulded into films using a hot press (George E Moore and Sons, Birmingham, UK) at 180°C and a pressure of 20 kN for 2 min. The resulting films were left to cool down to room temperature naturally. Neat PLLA films were processed similarly.

2.7. Characterisation of bacterial cellulose nanofibrils and its PLLA nanocomposites

2.7.1. Scanning electron microscopy (SEM)

SEM was performed using a high resolution field emission gun scanning electron microscope (LEO Gemini 1525 FEG-SEM, Oberkochen, D). It was used to characterise the composite microspheres, filter cakes for the direct wetting measurement and the morphology of the functionalised BC. The accelerating voltage used was 5 kV. To enable observation of the microsphere's interior the microspheres were frozen in liquid nitrogen and bisected using a scalpel. Prior to the SEM, all the samples were fixed onto SEM stubs using carbon tabs and Cr coated for 1 min at 75 mA.

2.7.2. Mechanical testing of nanocomposite films

Nanocomposite and neat PLLA films were cut into dog-bone shaped samples using a Zwick cutter (Zwick GmBH and Co. KG, Ulm, D). These dog bone shaped samples had an overall length of 75 mm, gauge length of 30 mm, thickness of 0.2 mm, the narrowest part of the sample was 4 mm. Tensile tests were conducted in accordance to BS EN ISO 527: 1996 using an Instron universal material testing machine (Instron 4502, Instron Corporation, MA, USA). The testing speed was 1 mm $min^{-1}$and load cell used 1 kN.

2.7.3. Effect of functionalised BC on the molecular weight of PLLA

The effect of the extrusion process with and without functionalised BC on the molecular weight of PLLA was investigated using gel permeation chromatography (GPC). The weight-averaged molecular weight (M_w) and polydispersity of PLLA were evaluated using conventional GPC with a refractive index detector and a PLgel 10 μm mixed bed-B column. Chloroform was used as the effluent at 30°C (flowrate was 10 mL min^{-1}). Prior to the injection, the nanocomposite and neat PLLA samples were dissolved in 10 mL of chloroform overnight and the solutions were filtered through a glass fibre pre-filter and a 0.2 μm polyamide membrane.

2.7.4. Differential scanning calorimetry (DSC) study of nanocomposites

The crystallisation and melting behaviour of the BC reinforced PLLA nanocomposites and neat PLLA were investigated using DSC (DSC Q2000, TA Instruments, UK) in He atmosphere. A sample mass of approx. 6 mg was used for each sample. A heat-cool-heat regime was applied in this measurement and the second heating curve used for thermal analyses. The sample was heated from 20°C to 210°C at a heating rate of 10°C min^{-1} before cooling it down to 20°C using a cooling rate of 50°C min^{-1}. The

sample was then re-heated to 210°C again at a heating rate of 10°C min^{-1}. The crystallinity of the nanocomposites produced was obtained from:

$$\chi_c(\%) = \frac{\Delta H_m}{\Delta H_m^{\circ} \times w} \times 100\% \quad [1]$$

where χ_c is the crystallinity, w is the weight fraction of PLLA in the composite, ΔH_m is the melting enthalpy from DSC and ΔH_m° is the melting enthalpy of pure crystalline PLLA (93.7 J g^{-1}) [32].

2.7.5. Thermal Gravimetry Analysis (TGA) of nanocomposites

The thermal degradation behaviour of the nanocomposites and neat PLLA was characterised using TGA (TGA Q500, TA Instruments, UK). A sample size of approx. 5 mg was used and the sample was heated from room temperature to 500°C at a rate of 10°C min^{-1}. A nitrogen atmosphere was used for this characterisation to provide an inert atmosphere.

2.7.6 Dynamic Mechanical Analysis (DMA) of the nanocomposites

The viscoelastic behaviour of the nanocomposites was characterised using DMA (Tritec 2000, Triton Technology Ltd, Keyworth, UK). DMA was performed in single beam cantilever bending mode with a gauge length of 10 mm. The sample has a width of 4 mm and an average sample thickness of 0.3 mm. The storage modulus, loss modulus and energy dissipation factor (tan δ) were measured from 30°C to 120°C using a heating rate of 5°C min^{-1}, with a frequency of 1 Hz.

3. Results and Discussions

3.1. Morphology of surface functionalised BC

Figure 1 shows the SEM images of the functionalised and neat BC. It can be seen that the BC nanofibrils were about 50 nm in width and several micrometres long. The functionalisation reaction did not seem to change the morphology of these nanofibrils. C_2-BC, C_6-BC and C_{12}-BC still possessed the same fibrous structure as seen in neat BC. This is an indication that the functionalisation occurred essentially on the surface but not the bulk of the nanofibrils. If the functionalisation occurred in the bulk, corresponding to a higher degree of substitution, the surface of the nanofibrils should not be smooth and damages to the fibre surface should be observed [33].

In addition to this, attenuated total reflection infrared (ATR-IR) spectroscopy (data not shown) showed the appearance of new carbonyl bonds (C=O) around 1750 cm^{-1}. This is a direct result of the esterification of BC. The absorbance band of hydroxyl groups (-OH) around 3300 cm^{-1} did not seem to decrease significantly. This suggests the reaction occurred on the surface of the BC rather then the bulk. Therefore, it was concluded that the functionalisation reaction essentially occurred on the surface of the nanofibrils.

3.2. Direct wetting measurements on functionalised BC

The direct wetting method was used as a simple means to determine the wettability of functionalised and neat BC nanofibrils by PLLA melts and thereby, quantifying the thermodynamic adhesion between single BC nanofibres and PLLA. Figure 2 shows examples of typical SEM images of a drop of PLLA melt on single BC nanofibre. From the measured contact angles (Table 1), it can be seen that as the chain length of the organic acid used to functionalise BC increased, the wettability between PLLA and the nanofibre increased. This is due to the fact that the esterification reaction introduced hydrophobic groups onto the surface of BC. The longer the hydrocarbon chain, the more hydrophobic the surface will become (water-air contact angles measured on BC and C_{12}-BC paper is 19°±7° and 133°±9°, respectively). The decrease in the contact angle between PLLA and BC indicates an increase in the adhesion between the polymer and the functionalised BC. From Young-Dupré's equation [34], it can be inferred that if the surface tension of the wetting liquid remains constant and the contact angle decreases, the work of adhesion increases. This will lead to a better interface between the liquid (polymer melt) and the substrate (functionalised BC). It should also be noted that this direct wetting method is in fact measuring the receding contact angle rather than the advancing contact angle as the polymer was first precipitated onto the nanofibre and then melted. This led to the de-wetting of the polymer from the surface of the nanofibre.

3.3. The use of composite microspheres for extrusion

As mentioned earlier, composite microspheres were produced to allow dry processing of BC reinforced polymer nanocomposites using a conventional extrusion process. Another main advantage of using this method is that it enables the dispersion of dry BC in the polymer melt. This method is also intrinsically scalable. In terms of the morphology of the composite microspheres, they were about 2.5 mm in diameter (Figure

3a). The diameter of these microspheres is highly dependent on the internal diameter of the tip of the syringe used to produce the spheres. These microspheres possess a porosity of approximately 94% (calculated from the polymer to solvent ratio). The porous spheres are shown in Figure 3b and their internal structure can be observed from the SEM image, Figure 3c. Voids can be seen in the microspheres (Figure 3b). This was due to the entrapment of air during the drop-wise addition of polymer solution into the liquid nitrogen bath. Similar observations have been reported in the literature [23, 35]. Figure 3c shows the structure of the composite microspheres at high magnification. The composite microspheres possess a channel-like structure. This can be attributed to the solvent freezing from the outside towards the centre of the microsphere. These channels represent the three-dimensional fingerprint of the solvent rich phase, which crystallised (froze) during phase separation. The structure of the composite microspheres was highly anisotropic (radially and axially), which is a characteristic of solid-liquid phase separation induced by TIPS process [36].

3.4. Mechanical properties of nanocomposites

The tensile modulus of all the nanocomposites increased when compared to neat PLLA (Table 2). The tensile modulus increased by as much as 50%, as seen in PLLA/C_{12}-BC (5 wt%). Based on the "rule of mixtures" for nanocomposites [37], the elastic modulus of a nanocomposite is the weighted mean of the elastic moduli of the polymer matrix and the reinforcement, depending only on the volume fractions and the orientation of the reinforcement. Since BC possesses a higher modulus compared to PLLA, the elastic modulus of the nanocomposites increases as expected when BC is incorporated into PLLA.

It can also be seen from Table 2 that the tensile strength of the nanocomposites improved by as much as 15% (PLLA/C_{12}BC 5 wt%). As a comparison, Huda et al. [38] have investigated the mechanical properties of recycled newspaper cellulose fibre (RNCF) reinforced PLLA composites. A fibre loading of 30 wt% was required to improve the tensile strength of the matrix by 15%. Such differences can be attributed to the large surface area of BC compared to RNCF. The improvements observed in the tensile strengths of the nanocomposites reinforced with functionalised BC could also be ascribed to the good dispersibility of functionalised BC in the polymer (the nanocomposites are transparent, Figure 4) and the intimate adhesion between functionalised BC and the polymer matrix.

Due to the hydrophilic nature of neat BC, the dispersibility of the nanofibrils in the hydrophobic polymer melt and the interfacial adhesion between BC and PLLA are poor [39]. Such effects reduce the ability to transfer stress from the matrix to the reinforcement and thereby limit the tensile strength of the nanocomposites. The surface hydrophobisation of BC improved the dispersibility of BC in the PLLA melt as well as the interfacial adhesion between BC and PLLA. As a result, the tensile strength of C_6-BC and C_{12}-BC reinforced nanocomposites showed significant improvements when compared to neat BC reinforced PLLA nanocomposites.

Although the direct wetting measurements showed lower contact angle (increased adhesion) between PLLA droplets and C_2-BC compared to neat BC, PLLA/C_2-BC nanocomposites exhibited lower tensile properties compared to PLLA/BC nanocomposites. Visually, PLLA/C_2–BC nanocomposite samples were brown in colour as compared to other nanocomposites, which are optically transparent (Figure 4). PLLA/C_2-BC nanocomposites also suffered from serious embrittlement when compared to the rest of the nanocomposite samples, including PLLA/BC. This might be due to the hydrolysis of the polymer matrix due to the incorporation of C_2-BC nanofibrils. The relative hydrophilic nature of C_2-BC (water/air contact angle of 75°±3°) compared to other functionalised BC and therefore, the presence of water might cause the hydrolysis of the ester bonds in C_2-BC during the extrusion at 180°C. The produced acetic acid will initiate the acid catalysed hydrolysis of PLLA [21], leading to a decrease in the molecular weight of the matrix, which was confirmed by GPC (Table 2). The lower molecular weight led to the lower tensile properties and the embrittlement of the nanocomposites. It should be noted that the measured molecular weight is an integral measure of the whole nanocomposites. The molecular weight surrounding C_2-BC might even be lower than that of the bulk of the matrix. Due to the hydrophobic nature of C_6-BC (advancing water/air contact angle of 92°±2°) and C_{12}-BC (advancing water/air contact angle of 133°±9°), less water will be absorbed by the nanofibrils and the hydrolysis of ester bonds will be negligible. Hence, the matrix still possessed its original molecular weight.

3.5. Crystallisation and melt behaviour of nanocomposites

The DSC curves are shown in Figure 5 and the characteristic temperatures such as glass transition temperature (T_g), crystallisation temperature (T_c) and melt temperature (T_m)

are tabulated in Table 3, along with the degrees of crystallinity of the nanocomposites. From Table 3, it can be concluded that the degree of crystallinity of PLLA was not significantly affected by the addition of BC into the matrix. The addition of BC nanofibrils into the matrix did however have a profound impact on the crystallisation behaviour of PLLA (Figure 5). It can be observed that T_c of the matrix decreased from 120°C to about 100°C in the presence of BC. This implied that the presence of BC aided the crystallisation of the matrix. A similar effect has been reported in the literature [32]. T_g and T_m of the nanocomposites on the other hand were not affected when compared to neat PLLA. This signifies that the BC did not affect the chain mobility of the polymer. The appearance of two melt peaks in neat PLLA is not surprising; annealing of a crystallisable PLLA will often produce two melt peaks [40]. An exotherm at around 150°C was also observed prior to the melting of PLLA in the nanocomposites samples. This exotherm is consistent with the solid-solid crystal transformation of the α' form to the α form of PLLA [41]. However, this exotherm was not observed in neat PLLA. This is because the α' form forms only below 120°C [42], which was the case for all the nanocomposites.

3.6. Thermal degradation behaviour of nanocomposites

The onset thermal degradation temperature (T_d) and the TGA curves of the neat polymer and its BC nanocomposites are shown in Table 3 and Figure 6, respectively. It can be seen from Table 3 that T_d increased for all the nanocomposites. All the composites underwent single step degradation (Figure 6). This increment in T_d and the improvements in the thermal stability of the nanocomposites indicated that the presence of BC does affect the thermal stability of the nanocomposites. Such results can be attributed to the interaction between BC and the matrix [43]. The low T_d observed for the PLLA/C_2-BC (2 wt%) nanocomposite sample might be a direct result of the lower molecular weight of the polymer matrix, which in turn reduced the thermal stability of the nanocomposites.

3.7. Viscoelastic behaviour of nanocomposites

Figure 7 and Figure 8 show the storage modulus and tan δ of the BC reinforced PLLA nanocomposites as a function of temperature. It is worth mentioning that these figures do not contain the DMA results for PLLA/C_2-BC (2 wt%). This is due to the brittleness of PLLA/C_2-BC (2 wt%). The sample failed repeatedly during the DMA runs (a total of 5 tries were made). Although the increment in storage moduli differs from sample

to sample (Figure 7) it can be seen that generally, the storage moduli of the nanocomposites are higher than that of neat PLLA. The use of BC to reinforce PLLA matrix resulted in a much stiffer material compared to the neat PLLA. This is a direct result of the reinforcing ability of BC. There are two possible contributions to the increment in the storage moduli [38]; (i) intramolecular bonds between BC and PLLA and (ii) rigid structure of BC.

The storage modulus of PLLA/C_2-BC (5 wt%) is significantly lower than other composites at 5 wt% loading fraction. This low value of storage modulus might be a direct consequence of the degraded (lower molecular) weight matrix (Table 2). It can also be seen that the storage moduli of the nanocomposites are higher than neat PLLA beyond its glass transition temperature at around 59°C (Figure 7). This is due to the early crystallisation of the polymer matrix. Such results corroborate the DSC results. T_c was found to be 120°C for neat PLLA compared to lower temperatures (by ~15°C) for the nanocomposites.

The tan δ of the neat polymer and nanocomposites as a function of temperature is shown in Figure 8. The tan δ peak was not significantly affected by the addition of BC. One reason might be the loading fraction was too low to have a profound impact on the mobility of the polymer chains. These results are in agreement with the absence of significant changes in T_g of the nanocomposites as measured by DSC. The mechanical T_g can be determined from the peak of tan δ or the point at which the storage modulus changes sharply. In this study, the mechanical T_g was taken as the peak of tan δ (Table 4). It can be seen that the mechanical T_g is about 8°C higher than the glass transition temperature determined by DSC. However, the changes in the mechanical T_g are not significant. Such results are not surprising as high loading fraction of reinforcement [38] or high crystallinity of the polymer matrix [32] is usually required to have a significant impact on the polymer chain mobility. The storage modulus increased by as much as 28% upon incorporation of BC (Table 4). Generally, the higher the loading fraction of BC, the larger the increment in the storage modulus, with the exception of C_{12}-BC reinforced nanocomposites. The exception seen in C_{12}-BC reinforced nanocomposites might be due to the good contact between the polymer and the reinforcement, which provides good stress transfer from the matrix to modified BC regardless of the loading fraction. However, the increase of storage modulus by C_{12}-BC reinforced PLLA nanocomposites was not as high as neat BC reinforced nanocomposites. One explanation is that the crystallinity as measured by XRD

of the BC is higher for neat BC (85%, data not shown) compared to C_{12}-BC (78%, data not shown).

4. Conclusion

The hydrophilic surface of BC was rendered hydrophobic by organic acid functionalisation. The degree of hydrophobicity can be tailored by the length of the organic acid (C_2 to C_{12}) used to modify the BC surface. The incorporation of organic acid functionalised BC into PLLA led to an improvement in both tensile modulus and tensile strength of the C_6-BC and C_{12}-BC reinforced nanocomposites (by as much as 50% and 15%, respectively). However, the PLLA nanocomposites reinforced by C_2-BC seemed to undergo acid catalysed hydrolysis during extrusion and this led to a decrease in the molecular weight of the PLLA, which in turn affected the mechanical properties of the resulting material. An increase in the thermal degradation temperature by 15°C was also observed for the nanocomposites compared to neat PLLA. The nanocomposites also exhibit higher storage moduli compared to neat PLLA. This is evidence of improved interfacial adhesion between the polymer matrix and the functionalised BC. This result was also confirmed measuring the contact angle between PLLA and BC. Therefore, it can be concluded that PLLA nanocomposites with overall improved properties can be fabricated through the surface functionalisation of BC.

Acknowledgments

The authors would like to thank Smithers Rapra Technology Ltd, Ms. Patricia Carry and Mr. Joseph Meggyesi for their help in the characterisation of the nanocomposites. We greatly acknowledge the funding provided by the UK Engineering and Physical Science Research Council (EPSRC) (EP/F032005/1) for KYL and the Challenging Engineering Programme of the EPSRC (EP/E007538/1) for funding JJB.

References

[1] Bismarck A. Are hierarchical composite structures the way forward to improve the properties of truly green composites? Express Polym. Lett. 2008; 2 (10): 687.
[2] Mohanty AK, Misra, M, Hincrichsen G. Biofibres, biodegradable polymers and biocomposites: An overview. Macromol. Mater. Eng. 2000; 276 (3-4): 1-24.
[3] Oksman K, Skrifvars M, Selin J-F. Natural fibres as reinforcement in polylactic acid (PLA) composites. Comp. Sci. Tech. 2003; 63 (9): 1317-1324.
[4] Juntaro J, Pommet M, Mantalaris A, Shaffer M, Bismarck A. Nanocellulose enhaced interfaces in truly green unidirectional fibre reinforced composites. Comps. Interface 2007; 14 (7-9): 753-763.

[5] Pickering KL, Beckermann, GW, Alam, SN, Foreman, NJ. Optimising industrial hemp fibre for composites. Comp. A 2007; 38 (2): 461-468.
[6] Nishino T, Hirao K, Kotera M. Kenaf reinforced biodegradable composite. Comp. Sci. Tech. 2003; 63 (9): 1281-1286.
[7] Plackett D, Andersen TL, Pedersen WB, Nielsen L. Biodegradable composites based on L-polylactide and jute fibres. Comp. Sci. Tech. 2003; 63 (9): 1286-1296.
[8] Juntaro J, Pommet M, Kalinka G, Mantalaris A, Shaffer MSP, Bismarck A, Creating hierarchical structures in renewable composites by attaching bacterial cellulose onto sisal fibers. Adv. Mater. 2008; 20 (16): 3122-3126.
[9] Pommet M, Juntaro J, Heng JYY, Mantalaris A, Lee AF, Wilson K, Kalinka G, Shaffer MSP, Bismarck A. Surface modification of natural fibers using bacteria: Depositing bacterial cellulose onto natural fibers to create hierarchical fiber reinforced nanocomposites. Biomacromolecules 2008; 9 (6): 1643-1651.
[10] Karnani R, Krishnan M, Narayan R. Biofiber-reinforced polypropylene composites. Polym. Eng. Sci. 1997; 37 (2): 476-483.
[11] Gindl W, Keckes J. Tensile properties of cellulose acetate butyrate composites reinforced with bacterial cellulose, Comp. Sci. Techn. 2004; 64 (15): 2407-2413.
[12] Suddel BC, Evans WJ. Natural fiber composites in automotive applications. In: Mohanty AK, Misra M, Drzal L. Natural fibers, biopolymers and biocomposites, CRC Press 2005.
[13] Ten Alps Communications Ltd t/a Sovereign Publications (2008), Rieter Automotive Systems, http://www.sovereign-publications.com/rieter.htm (accessed on 04.06.2009).
[14] Iguchi M, Yamanaka S, Budhiono A. Bacterial cellulose – a masterpiece of nature's art. J. Mater. Sci. 2000; 35 (2): 261-270.
[15] Czaja W, Romanovicz D, Brown RM. Structural investigations of microbial celllose produced in stationary and agitated culture. Cellulose 2004; 11 (3-4): 403-411.
[16] Hsieh YC, Yano H, Nogi M, Eichhorn SJ. An estimation of the Young's modulus of bacterial cellulose filaments. Cellulose 2008; 15 (4): 507-513.
[17] Bismarck A, Mishra S, Lampke T. Plant fibers as reinforcement for green composites. In: Mohanty AK, Misra M, Drzal L. Natural fibers, biopolymers and biocomposites, CRC Press 2005.
[18] Nakagaito AN, Iwamoto S, Yano H. Optically transparent composites reinforced with plant fiber-based nanofibers. Appl. Phys. A-Mater.; 81 (6): CP8-1112.
[19] Chanliaud E, Burrows KM, Jeronimidis G, Gidley MJ. Mechanical properties of primary plant cell wall analogues. Planta 2002; 215 (6): 989-996.
[20] Kim D-Y, Nishiyama Y, Kuga S. Surface acetylation of bacterial cellulose. Cellulose 2002; 9 (3-4): 361–367.
[21] Mochizuki M, Hirami M. Structural effects on the biodegradation of aliphatic polyesters. Polym. Advan. Technol. 1997; 8 (4): 203-209.
[22] Bhardwaj R, Mohanty AK. Advances in the properties of polylactides based materials: A review. J. Biobased Mater. Bioenergy. 2007; 1 (2): 191-209.
[23] Blaker JJ, Knowles JC, Day RM. Novel fabrication techniques to produce microspheres by thermally induced phase separation for tissue engineering and drug delivery. Acta Biomater. 2008; 4 (2): 264-272.
[24] Toyosaki H, Naritomi T, Seto A, Matsuoka M, Tsuchida T. Screening of bacterial cellulose-producing acetobacter strains suitable for agitated culture. Biosci. Biotech. Bioch. 1995; 59 (8): 1498-1502.
[25] Jandura P, Rieedl B, Kokta BV. Thermal degradation behaviour of cellulose fibers partially esterificed with some long chain organic acids. Polym. Degrad. Stabil. 2000; 70 (3): 387-394.
[26] Jandura P, Kokta BV, Riedl B. Fibrous long-chain organic acid cellulose esters and their characterisation by diffuse reflectance FTIR spectroscopy, solid-state CP/MAS C-13-NMR and X-ray diffraction. J. Appl. Polym. Sci. 2000; 78 (7): 1354-1365.

[27] Tran MQ, Cabral JT, Shaffer MSP, Bismarck A. Direct measurement of the wetting behaviour of individual carbon nanotubes by polymer melts: The key to carbon nanotube-polymer composites. Nano Lett. 2008; 8 (9): 2744-2750.
[28] Song BH, Bismarck A, Tahhan R, Springer J. A generalised drop length-height method for determination of contact angle in drop-on-fiber systems. J. Colloid Interf. Sci. 1998; 197 (1): 68-77.
[29] Kim Y, Jung R, Kim H-S, Jin H-J. Transparent nanocomposites prepared by incorporating microbial nanofibrils into poly(L-lactic acid). Curr. Appl. Phys. 2009; 9: S69-S71.
[30] Millon LE, Guhados G, Wan WK. Anisotropic polyvinyl alcohol-bacterial cellulose nanocomposite for biomedical applications. J. Biomed. Mater. Res. B 2008; 86B (2): 444-452.
[31] Ifuku S, Nogi M, Abe K, Handa K, Nakatsubo F, Yano H. Surface modification of bacterial cellulose nanofibers for property enhancement of optically transparent composites: Dependence on acetyl-group DS. Biomacromolecules 2007; 8 (6): 1973-1978.
[32] Mathew A P, Oksman K, Sain M. The effect of morphology and chemical characteristics of cellulose reinforcements on the crystallinity of polylactic acid. J. Appl. Polym. Sci. 2006; 101 (1): 300-310.
[33] Freire CSR, Silvestre AJD, Pascoal Neto C, Belgacem MN. Controlled heterogeneous modification of cellulose fibers with fatty acids: Effect of reaction conditions on the exten of esterification and fiber properties. J. Appl. Polym. Sci. 2006; 100 (2): 1093-1102.
[34] Shaw DJ. Introduction to colloid and surface chemistry 4th Ed. Butterworth-Heinemann 1992.
[35] Maquet V, Boccaccini AR, Pravata L, Notingher I, Jerome R. Porous poly(alpha-hydroxyacid)/Bioglass ® composite scaffolds for bone tissue engineering I: preparation and in vitro characterisation. Biomaterials 2004; 25 (18): 4185-4194.
[36] Schugens C, Maquet V, Granfils C, Jerome R, Teyssie P. Biodegradable and macroporous polylactide implants for cell transplantation 1: preparation of macroporous polylactide supports by solid-liquid phase separation. Polymer 1996l 37 (6): 1027-1038.
[37] Tibbetts GG, McHugh JJ. Mechanical properties of vapour-grown carbon fiber composites with thermoplastic matrices. J. Mater. Res. 1999; 14 (7): 2871-2880.
[38] Huda MS, Drzal LT, Mohanty AK, Misra M. Chopped glass and recycled newspaper as reinforcement fibers in injection molded poly(lactic acid) (PLA) composites: A comparative study. Comp. Sci. Tech. 2006; 66 (11-12): 1813-1824.
[39] Siqueira G, Bras J, Dufresne A. Cellulose whiskers versus microfibrils: Influence of the nature of the nanoparticle at its surface functionalisation on the thermal and mechanical properties of nanocomposites. Biomacromolecules 2009; 10 (2): 425-432.
[40] Bigg DM, Polylactide copolymers: Effect of copolymer ratio and end capping on their properties. Adv. Polym. Tech. 2005; 24 (2): 69-82.
[40] Kawai T, Rahman N, Matsuba G, Nishida K, Kanaya T, Nakano M, Okamoto HG, Kawada J, Usuki A, Honma N, Nakajima K, Matsuda M. Crystallisation and melting behaviour of poly(L-lactic acid). Macromolecules 2007; 40 (26): 9463-9469.
[42] Zhang JM, Tashiro T, Domb AJ, Tsuji H. Confirmation of disorder a form of poly(L-lactic acid) by the X-ray fiber pattern and polarized IR/Raman spectra measured for uniaxially-oriented samples. Macromol. Symp 2006; 242: 274-278.
[43] Nair KCM, Thomas S, Groeninckx G. Thermal and dynamic mechanical analysis of polystyrene composites reinforced with short sisal fibres. Comp. Sci. Tech. 2001; 61 (16): 2519-2529.

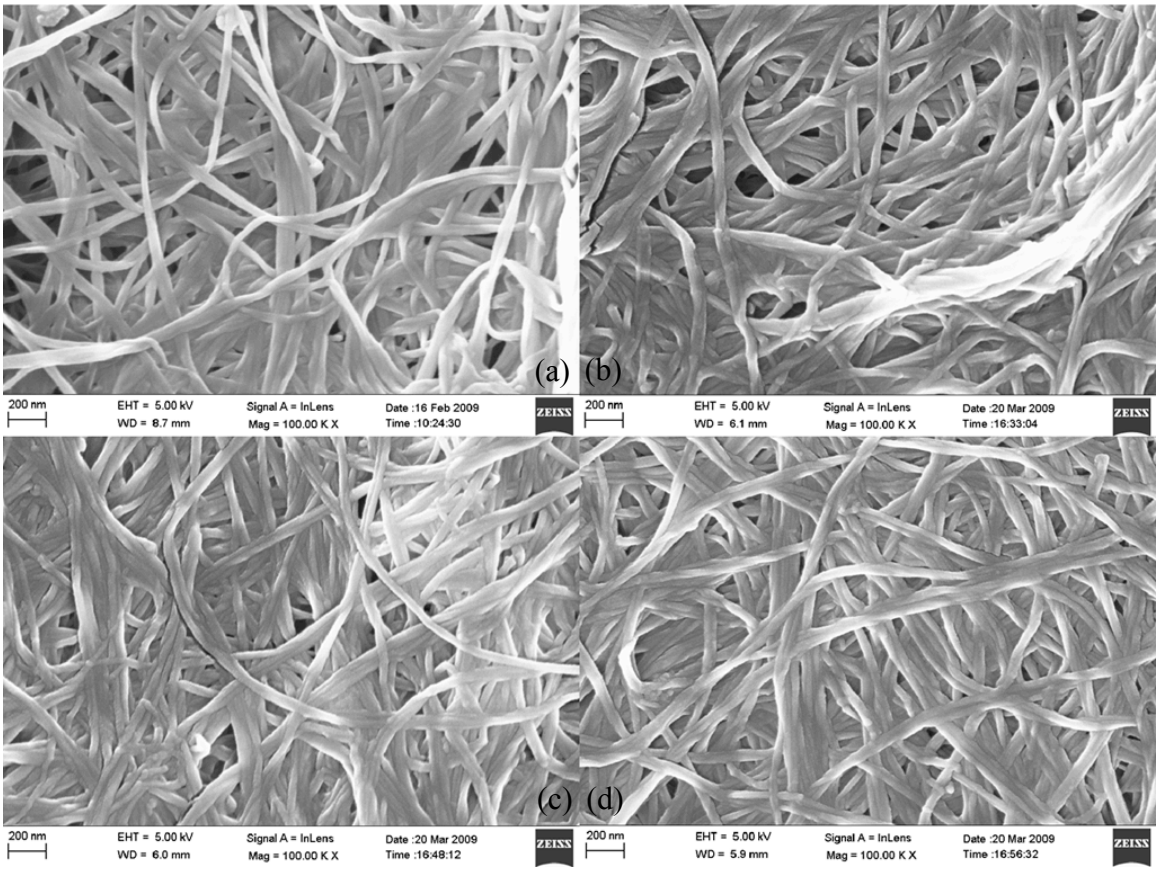

Figure 1: Scanning electron micrographs of (a) Neat BC, (b) C_2-BC, (c) C_6-BC, (d) C_{12}-BC

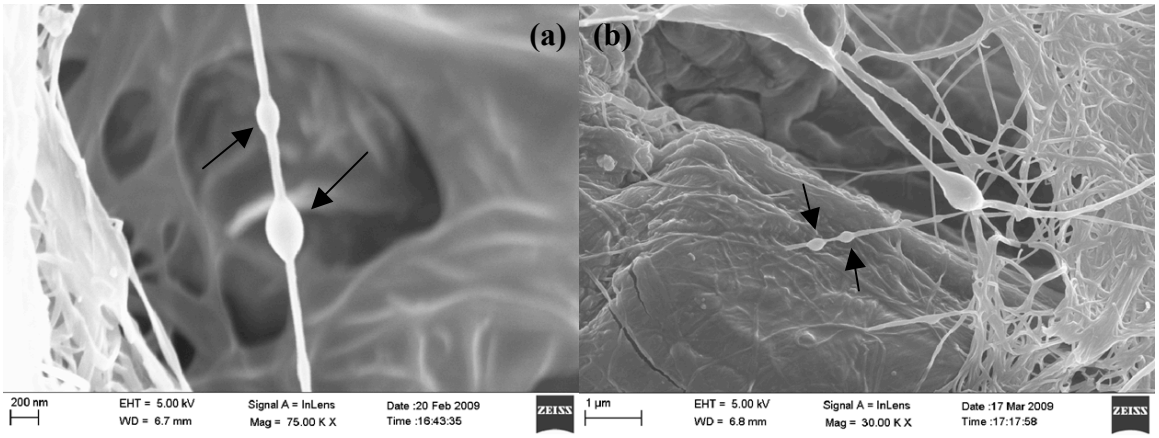

Figure 2: Typical examples of the SEM images showing PLLA melt droplets on BC nanofibre. (a) Neat BC, (b) C_{12}-BC.

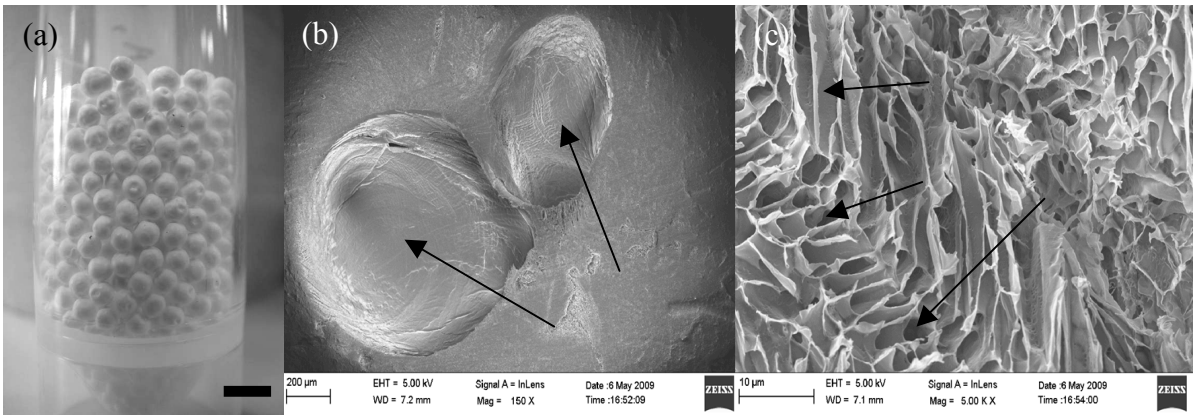

Figure 3: Images showing the morphology of BC/PLLA composite microspheres. (a) The microspheres, (b) SEM image of a microsphere at low magnification, (c) SEM image of a microsphere at high magnification. The scale bar on fig. 3(a) indicates 5 mm.

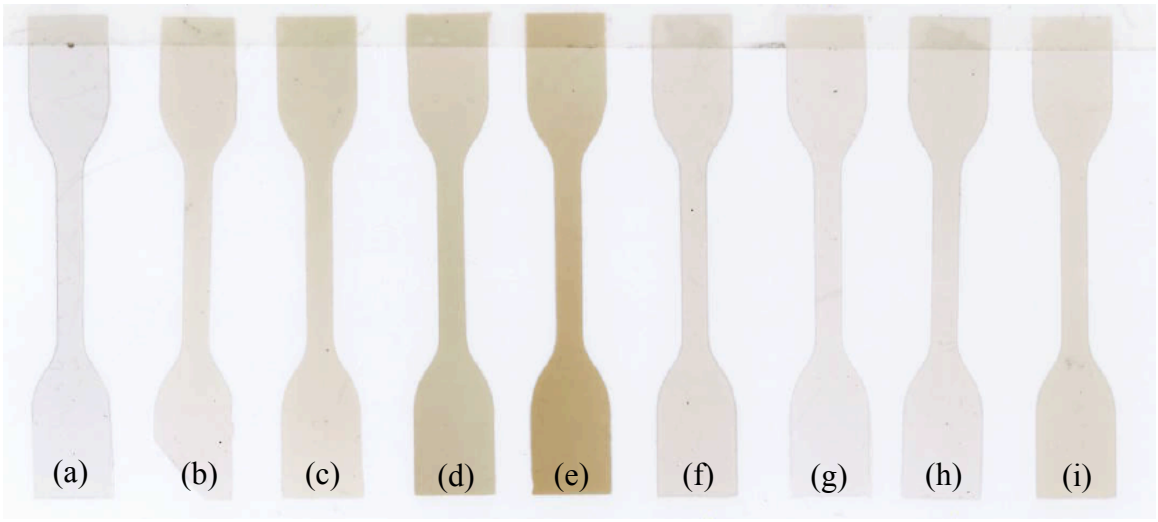

Figure 4: BC/PLLA nanocomposites samples. (a) Neat PLLA, (b) PLLA/BC (2 wt%), (c) PLLA/BC (5 wt%), (d) PLLA/C_2BC (2 wt%), (e) PLLA/C_2BC (5 wt%), (f) PLLA/C_6BC (2 wt%), (g) PLLA/C_6BC (5 wt%), (h) PLLA/C_{12}BC (2 wt%), (i) PLLA/C_{12}BC (5 wt%).

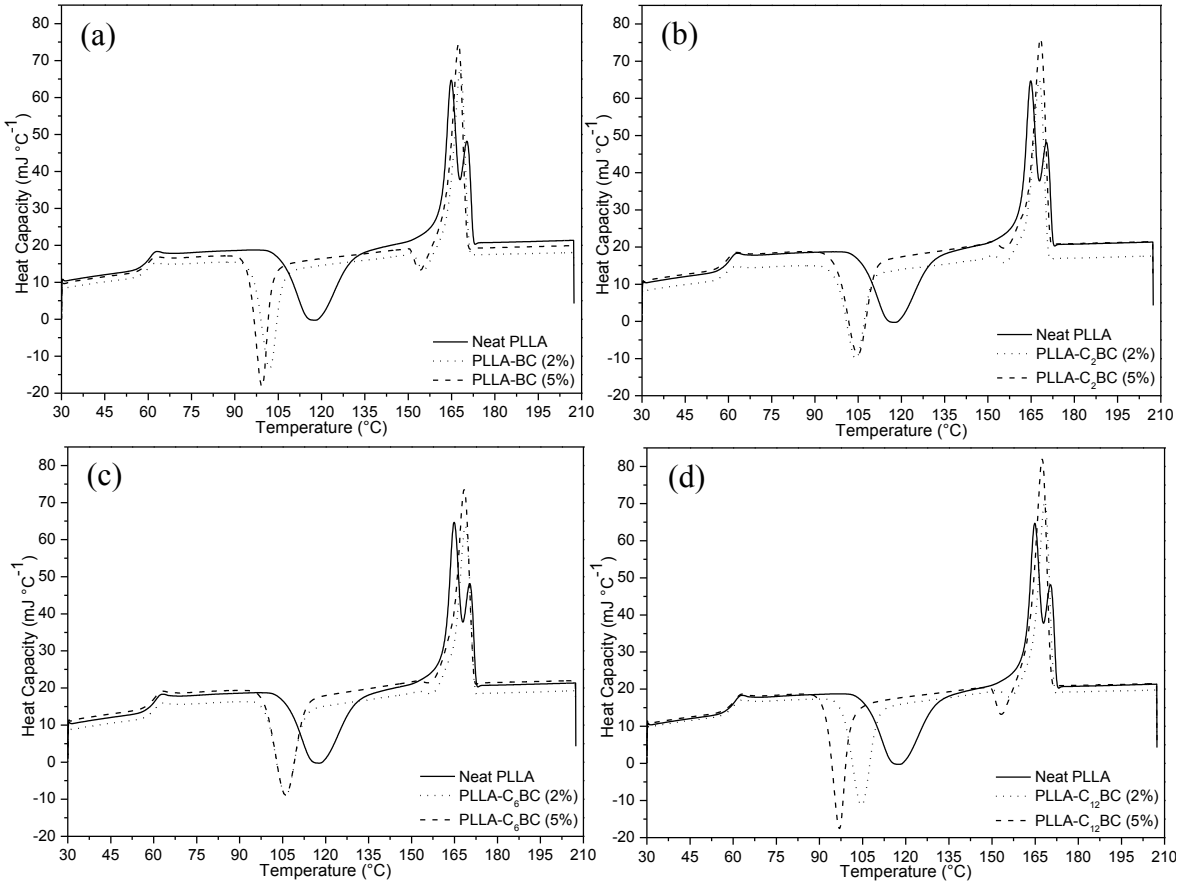

Figure 5: DSC plots of (a) PLLA/BC, (b) PLLA/C_2-BC, (c) PLLA/C_6-BC and (d) PLLA/C_{12}-BC nanocomposites.

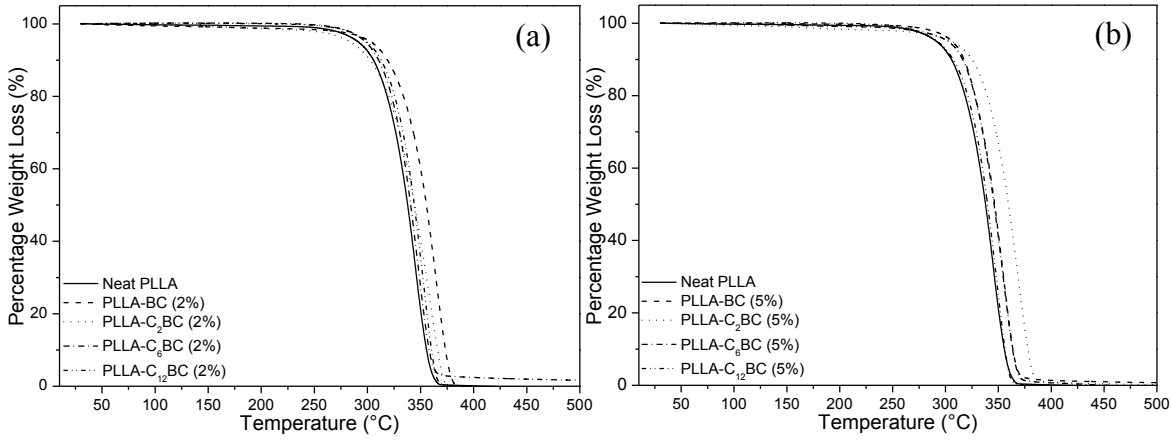

Figure 6: TGA curves of neat PLLA and its nanocomposites. (a) 2 wt% loading (b) 5 wt% loading.

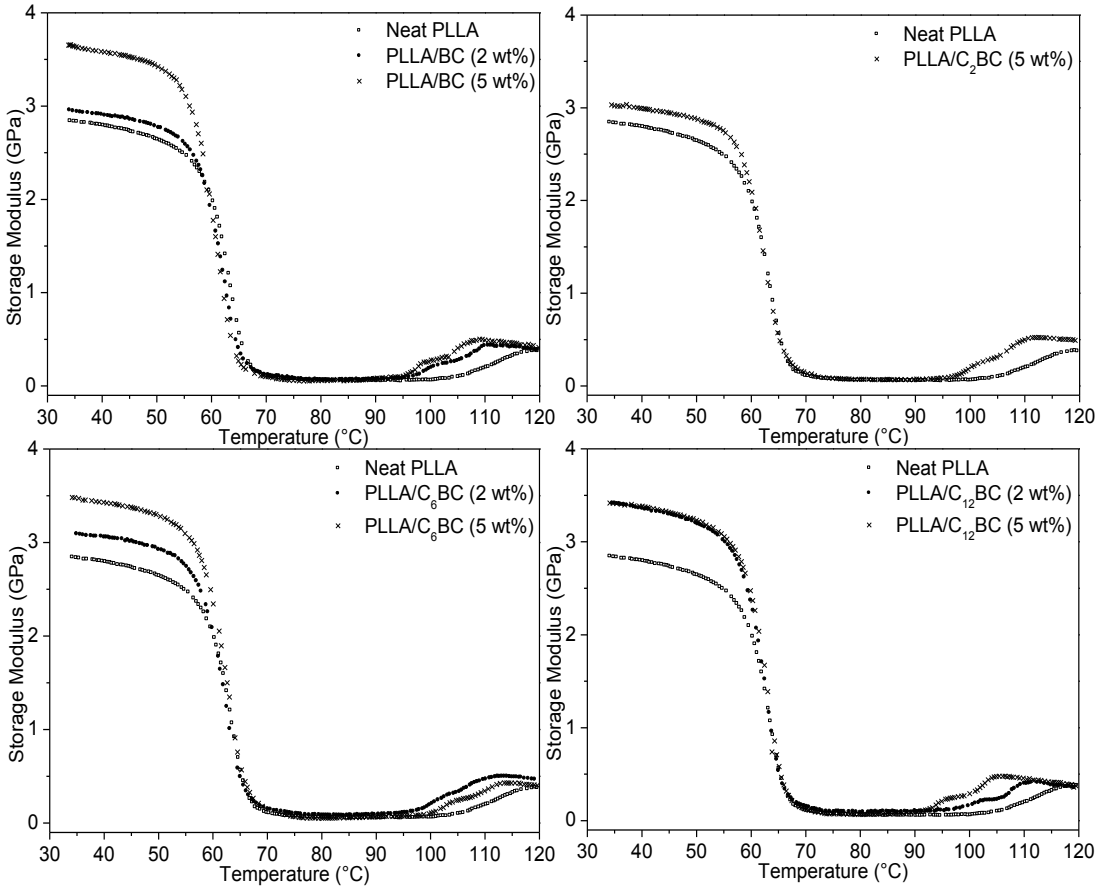

Figure 7: Storage modulus of neat PLLA and the nanocomposites with different functionalised BC nanofibrils and loading fractions.

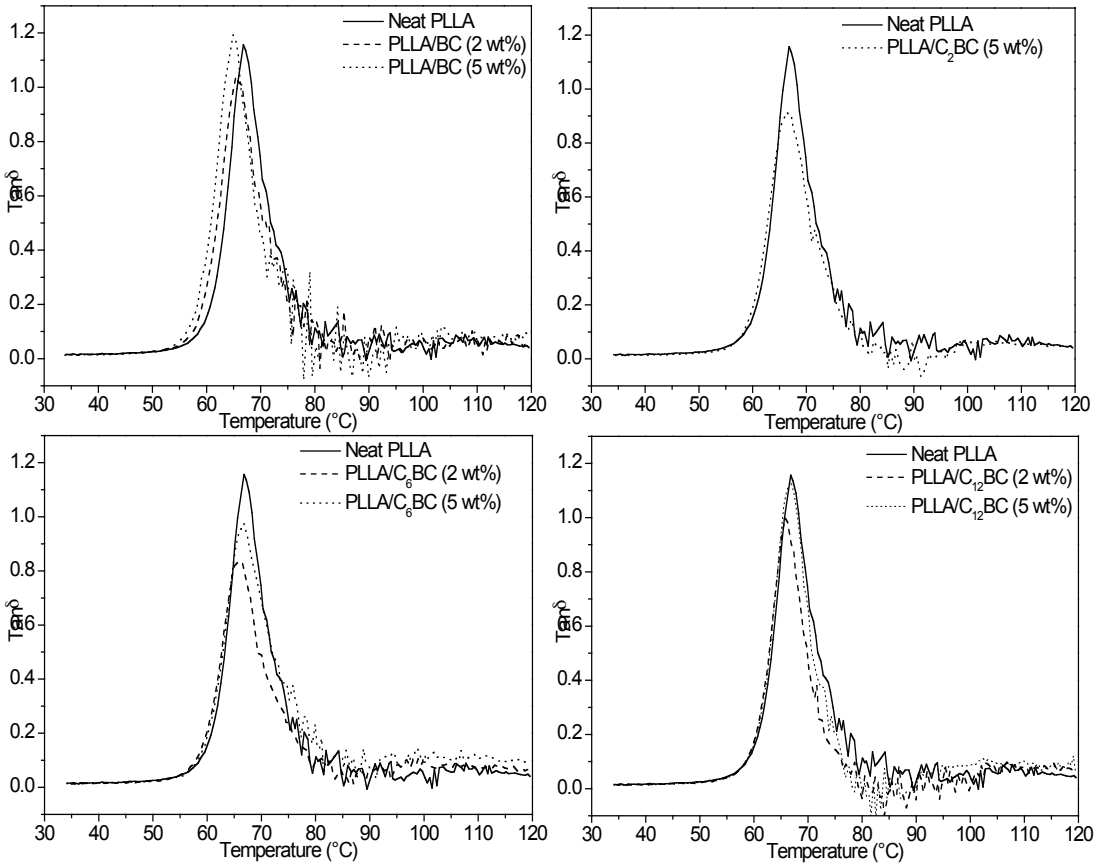

Figure 8: tan δ of the nanocomposites. (a) PLLA/BC, (b) PLLA/C_2-BC, (c) PLLA/C_6-BC, (d) PLLA/C_{12}-BC.

Table 1: Wettability of functionalised bacterial cellulose nanofibrils

Sample Name	Contact Angle (°)
Neat BC	35.4 ± 0.8
C_2-BC	29.5 ± 2.9
C_6-BC	27.7 ± 2.0
C_{12}-BC	20.8 ± 2.5

Table 2: Mechanical properties of cellulose nanofibrils reinforced PLLA nanocomposites

Sample	Tensile Modulus (GPa)	Tensile Strength (MPa)	Elongation at break (%)	M_w (kDa)
Neat PLLA	1.34 ± 0.04	60.7 ± 0.8	3.59 ± 0.07	157
PLLA/BC (2 wt%)	1.75 ± 0.05	57.5 ± 1.4	2.85 ± 0.12	147
PLLA/BC (5 wt%)	1.89 ± 0.02	60.9 ± 0.5	2.41 ± 0.08	146
PLLA/C_2BC (2 wt%)	1.71 ± 0.06	53.0 ± 1.4	2.23 ± 0.07	116
PLLA/C_2BC (5 wt%)	1.70 ± 0.03	60.1 ± 0.9	2.62 ± 0.07	135
PLLA/C_6BC (2 wt%)	1.63 ± 0.04	66.1 ± 2.4	3.12± 0.09	157
PLLA/C_6BC (5 wt%)	1.79 ± 0.02	65.1 ± 0.9	2.87± 0.03	153
PLLA/C_{12}BC (2 wt%)	1.66 ± 0.05	63.0 ± 1.2	3.21 ± 0.04	149
PLLA/C_{12}BC (5 wt%)	1.98 ± 0.04	68.5 ± 1.5	2.69 ± 0.06	157

Table 3: Glass transition temperature (T_g), crystallisation temperature (T_c), melt temperature (T_m), crystallinity (χ_c) and onset thermal degradation temperature (T_d) of functionalised PLLA nanocomposites

Sample	T_g (°C)	T_c (°C)	T_m (°C)	χ_c (%)	T_d (°C)
Neat PLLA	59	118	165 | 170	47.5	256
PLLA/BC (2 wt%)	59	102	168	46.0	275
PLLA/BC (5 wt%)	59	99	167	47.4	279
PLLA/C_2BC (2 wt%)	59	104	168	46.2	262
PLLA/C_2BC (5 wt%)	59	105	168	44.9	270
PLLA/C_6BC (2 wt%)	59	106	169	43.4	270
PLLA/C_6BC (5 wt%)	59	106	168	43.8	276
PLLA/C_{12}BC (2 wt%)	59	105	169	44.7	271
PLLA/C_{12}BC (5 wt%)	59	97	167	46.6	268

Table 4: Mechanical T_g, storage modulus (G') at 40°C, and the storage modulus imparted by the addition of BC nanofibrils

Sample	Mechanical T_g (°C)	G' @ 40°C (GPa)	G' @ 40°C imparted by nanofibrils (%)
Neat PLLA	67	2.79	-
PLLA/BC (2 wt%)	65	2.90	4
PLLA/BC (5 wt%)	65	3.58	28
PLLA/C_2BC (5 wt%)	66	2.99	7
PLLA/C_6BC (2 wt%)	66	3.06	9
PLLA/C_6BC (5 wt%)	67	3.42	23
PLLA/C_{12}BC (2 wt%)	66	3.35	20
PLLA/C_{12}BC (5 wt%)	67	3.38	21